Natural Resources, 2025, 16(11), 335-358
https://www.scirp.org/journal/nr
ISSN Online: 2158-7086
ISSN Print: 2158-706X

Water Use Regulation in Pre- and Post-Freeze *Avicennia germinans* Populations Reveal Mangrove Ecosystem Resilience

Cynthia Guo[1,2], Maria Ulatowski[1], Suvan Cabraal[1], Berit E. Batterton[3], Cleo Chiu[1], Ashley M. Matheny[1]

[1]Department of Earth and Planetary Sciences, Jackson School of Geosciences, The University of Texas at Austin, Austin, USA
[2]Department of Integrative Biology, College of Natural Science, The University of Texas at Austin, Austin, USA
[3]Department of Marine Science, Marine Science Institute, The University of Texas at Austin, Austin, USA
Email: jguo.cynthia@gmail.com

How to cite this paper: Guo, C., Ulatowski, M., Cabraal, S., Batterton, B.E., Chiu, C. and Matheny, A.M. (2025) Water Use Regulation in Pre- and Post-Freeze *Avicennia germinans* Populations Reveal Mangrove Ecosystem Resilience. *Natural Resources*, **16**, 335-358.
https://doi.org/10.4236/nr.2025.1611017

Received: September 26, 2025
Accepted: November 23, 2025
Published: November 26, 2025

Abstract

Mangrove forests provide critical ecosystem services, including coastline stabilization, habitats for marine life, and carbon storage. However, climate change introduces extreme temperatures and precipitation shifts that threaten their survival. The ability of mangroves to regulate their water use efficiently through plasticity in their hydraulic strategies will determine their resilience and capacity for range expansion. On the Texas coast, the northernmost range of the black mangrove *Avicennia germinans*, we investigated the short-term physiological responses to environmental fluctuations across the 2024 growing season, comparing juvenile mangroves that survived winter storm Uri in 2021 and saplings that established after the freeze event. From late spring to early fall, we measured leaf water potential, transpiration, carbon assimilation, and stomatal conductance and analyzed their relationships with temperature, vapor pressure deficit (VPD), photosynthetically active radiation (PAR), and salinity. We found that water use efficiency (WUE) was positively associated with variability in VPD at low VPD stress. *A. germinans* optimized carbon uptake while minimizing water loss during relatively higher VPD months through strategic regulation of stomatal conductance. Age class/disturbance history played only a small role in the mangroves' hydraulic responses to environmental stress. No significant WUE differences were observed between saplings and juveniles, suggesting consistent resilience across age classes and disturbance history. These findings indicate that *A. germinans* can maintain physiological stability under fluctuating conditions, supporting their long-term survival in a warming climate. Their ability to recover after extreme events, such winter storm Uri, underscores the potential for continued range expansion and mangrove ecosystem persistence in the Gulf of Mexico.

Keywords

Mangrove, Disturbance, Resilience, Ecohydrology, Vapor Pressure Deficit, Climate Change

1. Introduction

1.1. Background

Mangroves forests have historically been found in tropical and subtropical climates. However, in recent decades with rising average temperatures and milder winters associated with climate change, mangroves have gradually extended their ranges poleward into temperate latitudes [1] [2]. The black mangrove, *Avicennia germinans*, for example, has been expanding its range in the Gulf of Mexico extending as far north as the coasts of Texas, Louisiana, and Florida [3].

Mangroves in higher latitudes are faced with a variety of biotic and abiotic factors that limit their establishment, productivity, and resilience. Some of these factors include the rate of propagule dispersal and predation [4] and deep freeze events where air temperatures reach −6.3˚C to −7.6˚C or below [4] [5]. The Gulf of Mexico experiences a freeze regime that has historically been a major limiting factor in mangrove range expansion and has contributed to range contraction as freezes induce mass die-off events [6] [5]. One such event was caused by winter storm Uri in 2021 where air temperatures as low as −23˚C resulted in a mass die-off of *A. germinans* off the coast of Texas where we conducted our field study [7].

As mangroves attempt to establish further into the temperate zone, they must also adapt to the seasonal variations in temperature, humidity, and sunlight. This is in contrast with the tropics which experience variation in precipitation while maintaining consistently high temperatures, humidity, and sunlight levels year-round. Mangroves are known to be resilient in response to salinity, water pollution, and tidal undulation [8]-[10]. Their continued expansion, establishment, and population recovery after die-off events will depend in part on their ability to adapt their water regulation and stress response strategies to keep pace with the increased seasonal environmental variation and endure extreme weather events exacerbated by climate change (*i.e.* freezes, droughts).

1.2. Motivation

The purpose of this study was to increase our understanding of the plasticity of the hydraulic traits of black mangroves (*Avicennia germinans*) near Port Aransas, Texas to understand the resilience of the black mangrove forest ecosystems to environmental fluctuations as well as to analyze their post-disturbance recovery. We did so by examining their physiological responses to environmental forcings across the 2024 summer growing season, particularly in how they regulate water loss while maintaining photosynthesis. The timing of this study and local clima-

tology was such that the environment moved towards drier conditions as the summer progressed creating higher osmotic and atmospheric stress on the coastal vegetation.

All plants must manage their water content to survive. Water in plants influences their structural support, transport of materials, growth, productivity, and repair [11] [12]. Low water content puts vegetation at risk of potentially fatal embolisms which are obstructions in water flow caused by the buildup of air bubbles in the xylem [13] [14]. Trees manage water content in the root zone through water uptake and at the leaf level by controlling water loss to the atmosphere through their stomata. At the leaf level, closing stomata reduces water loss via transpiration at the expense of reducing atmospheric carbon uptake [15] [16]. Water regulation strategies vary by species and are influenced by xylem physiology, rooting habit, size, age, environment, disturbance history, and ecological conditions [17]-[19]. While most terrestrial plants are dependent on soil moisture for refilling their water content after transpirational loss during the day [20], mangroves grow in soils that are often fully saturated. Salinity, rather than soil saturation, therefore, is the greater limiting factor to the mangroves' ability to recover after water loss [18] [21]-[23].

Many studies have been conducted analyzing mangrove water regulation in response to salinity stress [18] [21]-[23]. However, few studies have been conducted analyzing plasticity in mangrove hydraulic traits in relation to a variety of ambient field conditions and disturbance histories. In this study, we focused on water regulation strategies of pre- and post-freeze black mangroves at the leaf level.

1.3. Hypothesis

Mangroves respond to changes in their environment by adapting their water regulation strategies at the leaf level by opening and closing stomata to maximize carbon uptake while attempting to minimize water lost to transpiration. We hypothesize that as temperature and VPD increase, increasing the evaporative forcing of the atmosphere, the transpiration, stomatal conductance, and assimilation rate will also decrease as the leaves close their stomata to prevent excessive water loss. We predict that leaf water potential will become more negative during these times corresponding to greater plant stress. We also predict that saplings (younger, established post-freeze) will have a higher WUE than juveniles (older, established pre-freeze) due to the saplings' narrower xylem vessels [24] and lower salt tolerance [23] leading to lower water content.

Several studies have shown differences in traits and physiological responses to the environment between age classes in different species of mangroves. Osland *et al.* (2015), for instance, found that after a freeze event in 2014 in Florida, adult *A. germinans* sustained less damage than juvenile mangroves, but seedlings remained mostly undamaged [25]. Kodikara *et al.* (2017) found that after the 15th to 20th week post-establishment, there is a shift toward higher optimal salinity for growth for five mangrove species, including two *Avicennia* species [23]. Cisnero

de la Cruz *et al.* (2021) observed a difference in xylem vessel size and density between adult and seedlings in the mangrove species *Rhizophora mangle* and found that leaf water potential was higher in saplings than in adults [24].

1.4. Implications

We conducted this study on the surviving population of *A. germinans* affected by winter storm Uri in 2021. The living trees we measured were young survivors of the freeze (juveniles) or post-freeze regenerations (saplings). This study therefore provides an understanding of the hydraulic trait plasticity of the surviving mangrove population about three years post-disturbance as well as points to potential differences between trees that survived the freeze as saplings and those that were established after.

Understanding how age class, especially the sapling stage, might affect hydraulic strategies will also improve our understanding of their establishment capabilities and ability of the population to recover after ecosystem disturbances. As mangroves encroach into new wetland ecosystems, we can use this data to predict their success in competition with the resident dominant forb vegetation. Changes in wetland vegetation habitats could induce wildlife composition changes [26].

Evapotranspiration also plays a significant role in atmospheric cooling by converting incoming solar radiation to latent heat rather than sensible heat. Vegetation cover therefore greatly influences regional heat fluxes and energy balances [27] [28]. With mangroves covering about 147,000 km^2 of the earth surface according to the GMW v4.0 world map developed by the Global Mangrove Watch [29], understanding how these trees adapt their transpiration rates in response to environmental fluctuations will contribute to greater accuracy in modeling regional climate and weather patterns in areas with large mangrove forest cover.

While mangroves are continuing to expand their range into the temperate zone, mangrove ecosystems globally are facing considerable threats to their existence from natural disasters, climate change, coastal development, aquaculture, and over-exploitation among other threats [30] [31]. According to an assessment by the IUCN Red List of Ecosystems, 50% of mangrove ecosystems in the assessment were categorized as Vulnerable, Endangered, or Critically Endangered [32]. Mangrove forests provide many ecosystem services including phytoremediation, which in some cases, protect more vulnerable habitats, such as coral reefs, from pollution damage [9] [33]. They also provide habitats and nurseries for marine and terrestrial wildlife [34], act as large carbon sinks [35]-[37] and protect against coastal erosion and flooding [10] [38]. Understanding questions of mangrove hydraulic trait plasticity and resilience in the face of changing conditions will inform conservation efforts and priorities.

2. Methods

2.1. Data Collection

We collected field measurements during monthly 2-to-3-day campaigns during

the summer of 2024. Measurements were conducted in May, July, September, and October. Our field site was located at Coyote Island (27.806 N, 97.09 W) near Port Aransas on the mainland facing side of Mustang Island, a barrier island along the south Texas coast. Port Aransas, Texas is within the northernmost part of the range of *A. germinans*.

Our site was located at sea level where high tide flooding of the land occurred. Black mangroves (*Avicennia germinans*) lined the edge of the land-ocean interface. We divided the mangrove zone at our site into three distinct sections about 20 meters long (Figure 1). Within each section, we made transects from the beginning of the vegetation line on the inland side to the end of the vegetation line on the ocean side using 1-meter quadrats. We counted the number of saplings and juveniles in each transect and calculated the ratio.

Figure 1. Transect example from section 2 of field data collection showing one-meter quadrats from the beginning of the vegetation line on the inland side (left) to the end of the vegetation line at the water (right).

We defined post-freeze sapling as a tree under 65 cm with 3 or fewer main stems and with small and few branches. We defined pre-freeze juveniles as a tree over 65 cm with more than 3 main stems and with extensive, long branching. This size-based classification is used as a proxy for pre- or post-freeze status and carries the potential for misclassification (e.g., a fast-growing post-freeze tree being classified as a juvenile). We did not sample trees more than a meter tall as all adult trees in this location experienced mortality in the freeze in 2021.

For each campaign, we took measurements during the following sampling periods throughout the day: pre-dawn (5:00 - 7:30 am), morning (7:30 - 11:00 am), midday (11:00 am - 1:30 pm), afternoon (1:30 - 5:00 pm), and evening (after 5:00 pm). During each sampling period, we took measurements from 1 - 2 juvenile tree leaves and 1 - 2 sapling tree leaves from each section resulting in 3 - 4 leaf meas-

urements per section per sampling period or 9 - 12 measurements per sampling period.

For each leaf, we used a LI-6800 Portable Photosynthesis System [39] to measure transpiration rate (the rate at which water leaves the leaf), assimilation rate (photosynthetic rate), and stomatal conductance (the rate of gas exchange through the stomata). We ran system warmups on the instrument before use every day that measurements were taken. For all measurements, the environment setting was set to fan on 5000 rpm, flow at 600 μmol s^{-1}, and humidity at 50%. CO_2 was set to the approximate ambient value of 420 ppm, and PAR was adjusted during each measurement session to match the ambient PAR conditions. Infrared gas analyzers (IRGAs), used to measure CO_2 and H_2O fluxes, were matched before each measurement session. Generally, we removed a branchette from the tree around two inches from the petiole to take the measurement of the leaf. We made leaf gas exchange measurements for morning through evening but excluded LI-6800 measurements during pre-dawn due to the lack of sunlight to drive photosynthesis.

Immediately after taking a LI-6800 measurement of any given leaf sample, we used a pressure chamber [40] to measure leaf water potential, expressed in units of pressure, megapascals (MPa), on the same sample before it had time to desiccate. Leaf water potential (LWP) serves as a proxy for plant stress. A more negative LWP signifies lower water availability in the leaves and greater plant stress. Leaf water availability directly impacts the turgor pressure exerted against plant cell walls which maintains the structure and rigidity of the plant [41]. We measured LWP from pre-dawn to evening. For each measurement, we recorded the exact time in which the final measurement was produced for both the gas flow using the LI-6800 system and the LWP using the pressure chamber.

We took three soil cores from the top 10 cm of sediment at the root zone of the mangroves during each campaign and analyzed their pore water salinity. Using a chilled centrifuge [42], we separated the pore water from the soil and analyzed its salinity using an optical salinity refractometer [43].

Precipitation, temperature, vapor pressure deficit (VPD), and photosynthetically active radiation (PAR) data were taken from ERA5-land hourly from Google Earth Engine [44] and resampled to the minute to match the exact time of each leaf measurement.

2.2. Analysis

For each month, we found the average and standard deviation for each metric we measured (transpiration (E), assimilation (A), stomatal conductance (g_{sw}), and leaf water potential (LWP)) for both sapling and juveniles. We tested for significant differences in the data sets for each metric between age groups (using an independent type 3, 2 tailed t-test) and between months. For all monthly comparisons, equal variance and/or normality ANOVA assumptions were violated. Therefore, we proceeded to analyze our monthly data with the non-parametric Kruskal-

Wallis test followed by the Dune's Test Pairwise Comparisons if a significant difference between months was identified.

2.3. Water Use Efficiency

Water use efficiency is the amount of carbon a plant can intake per unit of water lost. We calculated water use efficiency (WUE) using the following equation:

$$WUE = A/(E * 1000)$$

$$A = assimilation\ (\mu mol/m^2/s)$$

$$E = transpiration\ (mol/m^2/s)$$

$$WUE = water\ use\ efficiency\ (g\ of\ CO_2/g\ of\ H_2O)$$

We calculated the WUE for each measurement. We compared WUE across age class for each month using independent t-tests. We calculated the mean and standard deviation of WUE across the months for each age class. Then using the aggregated data sets (combining juvenile and sapling data) we conducted Kruskal-Wallis test paired with a Dune's Test Pairwise Comparison to determine differences in WUE across the four months.

2.4. Comparison to Environmental Data

We determined the trends for change in temperature, precipitation, VPD, and PAR across the four months and compared them with the corresponding trends in E, A, g_{sw}, LWP, and WUE.

We conducted linear regressions between each of three environmental factors (temperature, VPD, PAR) and each of the four vegetation metrics (E, A, g_{sw}, LWP). We calculated the p-value and R-squared value for each regression to determine significant relationships as well as determine which environmental factor had the greatest influence on mangrove water regulation strategies.

3. Results

In total, we took 159 measurements: 40 in May, 31 in July, 39 in September, and 49 in October. Variation in sample sizes between months are due to instrument failure or excluded observation errors. Data samples from all metrics (E, A, g_{sw}, LWP) failed either the equal variance and/or normality assumption for the ANOVA test. Therefore, we proceeded to analyze differences using the Kruskal-Wallis test and subsequently, the Dune's Test Pairwise Comparison.

Between juveniles and saplings, there was no significant difference in average LWP for May, July, or September. In October, there was a significant difference (p-value < 0.05) in average LWP during predawn but not during midday. Midday LWP values were on average lower (more negative) than those of predawn, signifying lower water availability in the leaf as the day progressed in all months (**Figure 2**).

For predawn LWP, the results of the Kruskal-Wallis test were an H-statistic of 13.16 and a p-value < 0.005 signifying a significant difference between two or more

months. A Dune's Test Pairwise Comparison showed that LWP predawn was significantly lower in October than in the other three months (Figure 2, panel A).

For midday LWP, the Kruskal-Wallis test produced an H-statistic of 23.78 and a p-value < 0.001 signifying a significant difference between two or more months. A Dune's Test Pairwise Comparison showed that midday LWP was significantly lower in July than in the other three months (Figure 2, panel B).

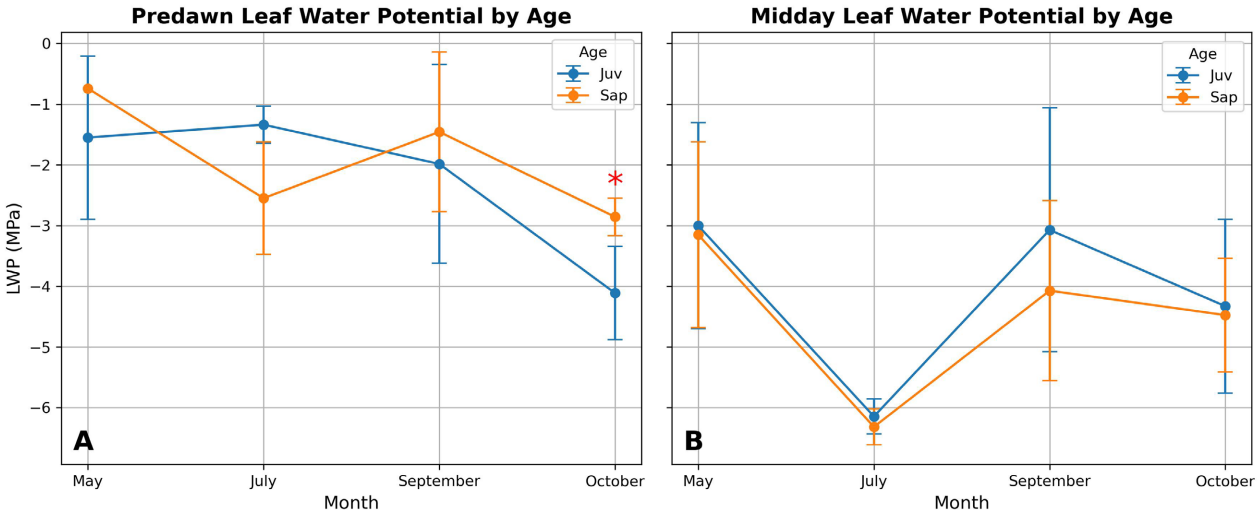

Figure 2. Comparison of predawn (A) and midday (B) leaf water potential (megapascals) across four months. Increasingly negative values signifies lower leaf water availability. Orange lines represent saplings, and the blue lines represent juveniles. The dot at each month represents mean values, and the error bars represent standard deviation for each month. The red star represents a significant difference between juvenile and sapling values in that month.

There was no significant difference in midday transpiration rate between juveniles and saplings for all four months. May and July saw similar rates of midday transpiration around 0.002 mol m^{-2} s^{-1}, while September saw a spike up to around 0.007 mol m^{-2} s^{-1}. October transpiration values returned to similar levels seen in May and July at 0.001 mol m^{-2} s^{-1} on average (Figure 3, panel A).

For midday transpiration, the Kruskal-Wallis test produced an H-statistic of 24.94 and a p-value < 0.001 signifying a significant difference between two or more months. A Dune's Test Pairwise Comparison showed that midday transpiration was significantly higher in September than in the other three months. October midday transpiration was also significantly lower than May (Figure 3, panel A).

There was a similar trend in stomatal conductance to transpiration across the four months with May, July, and October experiencing similar average stomatal conductance rates around 0.76 mol m^{-2} s^{-1} and a spike in September at an average of 0.28 mol m^{-2} s^{-1}. As with transpiration, there was no significant difference in stomatal conductance between age classes for all four months (Figure 3, panel B).

For midday stomatal conductance, the Kruskal-Wallis test produced an H-statistic of 27.81 and a p-value < 0.001 signifying a significant difference between two

or more months. A Dune's Test Pairwise Comparison showed that midday stomatal conductance was significantly different between May and July, May and October, July and September, and September and October. Between May and September there is a near significant difference with a p-value of 0.067 (**Figure 3**, panel B).

Assimilation rate, however, followed a slightly different trend than seen in both transpiration and stomatal conductance. Both juveniles and saplings experienced a spike in CO_2 assimilation in September, but while sapling assimilation decreased again in October (though not to the degree of change seen in transpiration or stomatal conductance), juvenile assimilation remained at a similar rate as seen in September. Therefore, in October, juveniles had a significantly higher CO_2 assimilation rate around 16 μmol m^{-2} s^{-1} than saplings at 8 μmol m^{-2} s^{-1} while there was no significant difference between age classes in May, July, or September (**Figure 3**, panel C).

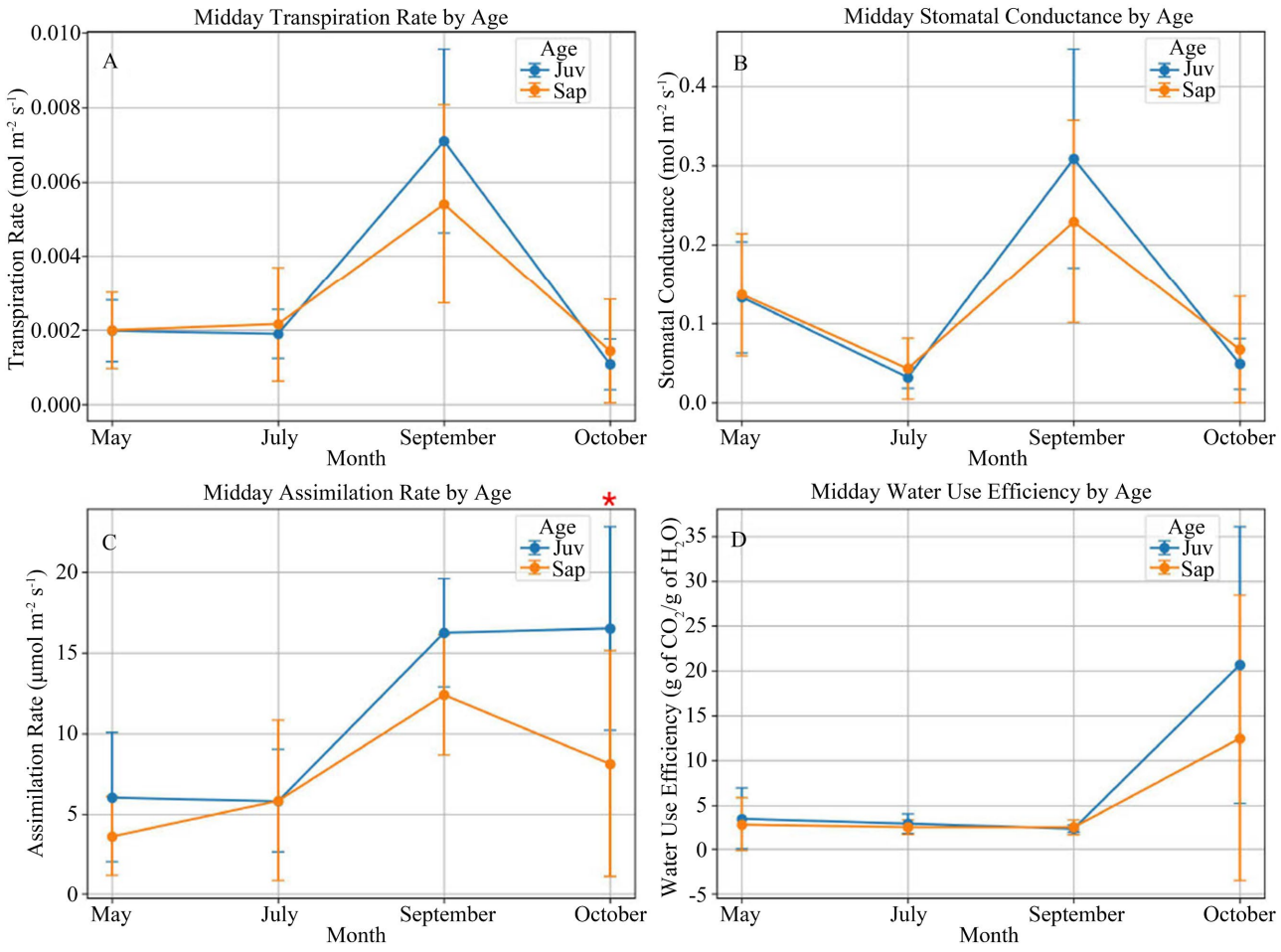

Figure 3. Comparison of midday transpiration (A), stomatal conductance (B), assimilation (C), and water use efficiency (D). Orange lines represent saplings, and the blue lines represent juveniles. The dot at each month represents mean values, and the error bars represent standard deviation for each month. The red asterisk represents a significant difference between juvenile and sapling values in that month.

For midday assimilation, the Kruskal-Wallis test produced an H-statistic of 19.19 and a p-value < 0.001 signifying a significant difference between two or more months. A Dune's Test Pairwise Comparison showed that midday assimilation was overall significantly higher in September and October than in May and July (Figure 3, panel C).

We calculated water use efficiency (WUE) for all measurements. We found no significant difference in midday WUE between juveniles and saplings for all months. WUE remained stable at around 2.5 g of CO_2/g of H_2O for May, July, and September but spiked to an average of 17.8 g of CO_2/g of H_2O in October (Figure 3, panel D).

For midday WUE, the Kruskal-Wallis test produced an H-statistic of 21.26 and a p-value < 0.001 signifying a significant difference between two or more months. A Dune's Test Pairwise Comparison showed that midday WUE was significantly higher in October than in the other three months (Figure 3, panel D).

The raw hourly temperature, VPD, and PAR data from ERA5 failed all assumptions of equal variance and normality.

The Kruskal-Wallis test for temperature in May, July, September, and October yielded an H-statistic of 1280.69 and a p-value < 0.001, indicating a highly significant difference in temperature between two or more months. The Dunn's Test Pairwise Comparison showed temperature varied significantly between all four months. A comparison of the mean temperature for each month showed the highest temperature in July and the lowest in October (Figure 4). The average, maximum, and minimum temperature for each month is shown in Table 1.

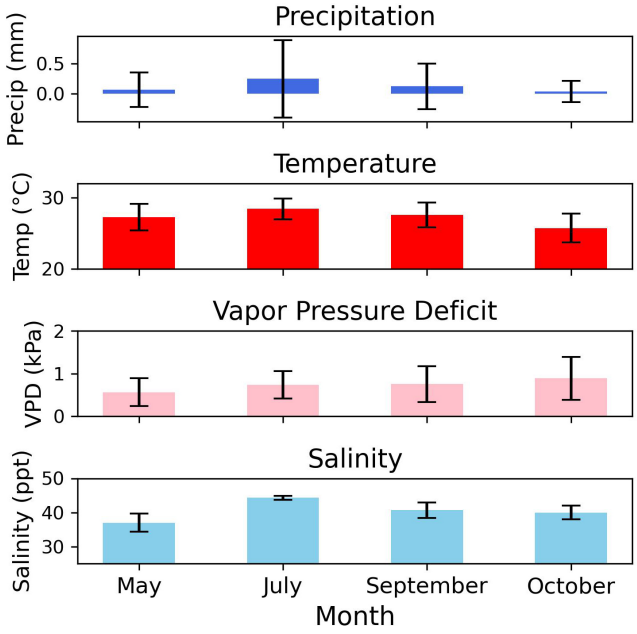

Figure 4. Meteorological data (precipitation, temperature, VPD) for four months in the summer of 2024 extracted from ERA5 land hourly from google earth engine and averaged for each month with error bars for standard deviation. Average salinity values are from pore water samples taken the days when leaf measurements were conducted.

Table 1. Maximum, minimum, and mean values for precipitation, temperature, VPD, PAR, and salinity for May, July, September, and October of 2024. Panel (A) details the environmental data from all the days of each month while panel (B) only pulls the environmental data from the two to three days we took field measurements each month.

(A) Full Month Environmental Data					
		May	July	September	October
Precipitation (mm)	mean	0.07	0.25	0.12	0.04
	max	6.21	6.47	3.82	2.74
	min	0	0	0	0
Temperature (C)	mean	27.28	28.43	27.57	25.75
	max	31.69	32.51	31.75	30.91
	min	22.57	24.66	23	20.64
VPD (kPa)	mean	0.56	0.74	0.75	0.89
	max	2.25	1.97	2.42	2.61
	min	0.05	0.15	0.14	0.04
PAR (μmol $m^{-2}s^{-1}$)	mean	475.16	114.68	368.96	350.33
	max	2066.58	517.53	1585.87	1516.9
	min	0	0	0	0
(B) Measurement Period Environmental Data					
		May	July	September	October
Precipitation (mm)	mean	0.08	0.01	0.1	0
	max	0.22	0.04	0.31	0
	min	0	0	0	0
Temperature (C)	mean	26.98	30.44	29.18	24.94
	max	27.84	31.31	30.47	27.38
	min	25.08	27.91	27.29	20.95
VPD (kPa)	mean	0.58	1.2	0.9	1.45
	max	0.85	1.48	1.22	1.84
	min	0.23	0.56	0.39	0.85
PAR (μmol $m^{-2}s^{-1}$)	mean	934.97	no data	793.66	564.09
	max	1779.46	no data	1425.17	968.46
	min	190.73	no data	0	0
Salinity (ppt)	mean	37	44.33	40.67	40
	max	40	45	42	42
	min	35	44	38	38

The Kruskal-Wallis test for VPD yielded an H-statistic of 432.08 and a p-value < 0.001 indicating a significant difference in VPD between two or more months.

The Dunn's Test Pairwise Comparison showed VPD varied significantly between all four months except between July and September. VPD increased gradually from the lowest in May to the highest in October (Figure 4). The average, maximum, and minimum VPD for each month are shown in Table 1.

The Kruskal-Wallis test for PAR yielded an H-statistic of 81.82 and a p-value < 0.001 indicating a significant difference in PAR between two or more months. The Dunn's Test Pairwise Comparison showed PAR varied significantly between May and September and May and October. The average, maximum, and minimum PAR value for each month is shown in Table 1.

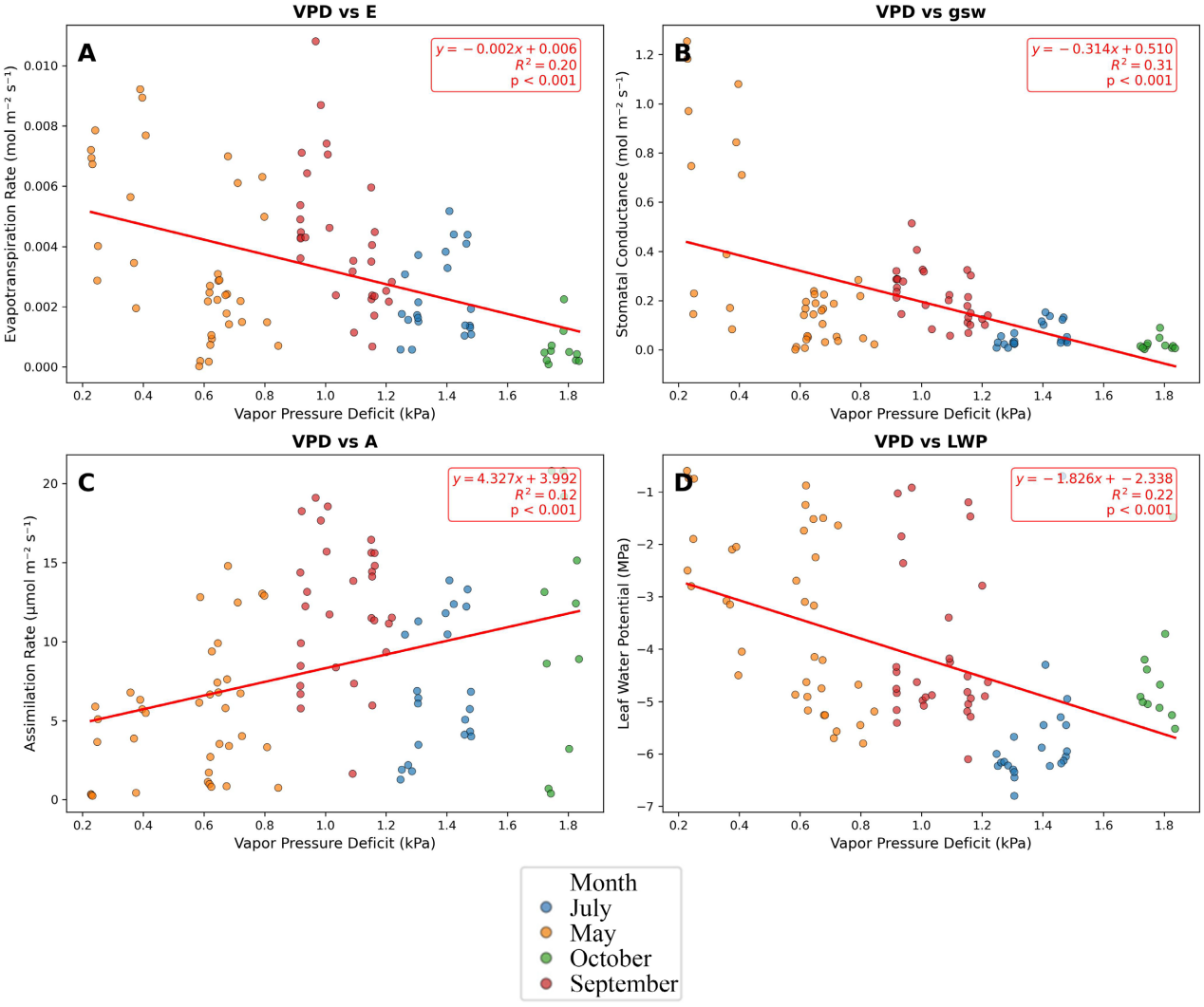

Figure 5. Vapor pressure deficit (VPD) was extracted from ERA5 land hourly from google earth engine and resampled to minutes. VPD values were paired with leaf measurements by time. Scatterplots depict VPD against transpiration (A), stomatal conductance (B), assimilation (C), and leaf water potential (D). The red line is the regression line indicating a significant relationship where the p-value is less than 0.05. The R-squared value, p-value, and trend line equation are represented in the red box at the top right corner of each graph. Blue dots represent July, orange represents May, green represents October, and red represents September.

According to the linear regression analysis between VPD and transpiration,

VPD explained about 20 percent of the variation in transpiration rate with a p-value < 0.001. There was a significant negative trend (y = −0.002x + 0.006) between VPD and transpiration (Figure 5, panel A).

VPD explained about 31 percent of the variation in stomatal conductance with a p-value < 0.001. There was a significant negative trend (y = −0.314x + 0.510) between VPD and stomatal conductance. May experienced the greatest variation in stomatal conductance while in all other months stomatal conductance remained relatively consistent (Figure 5, panel B).

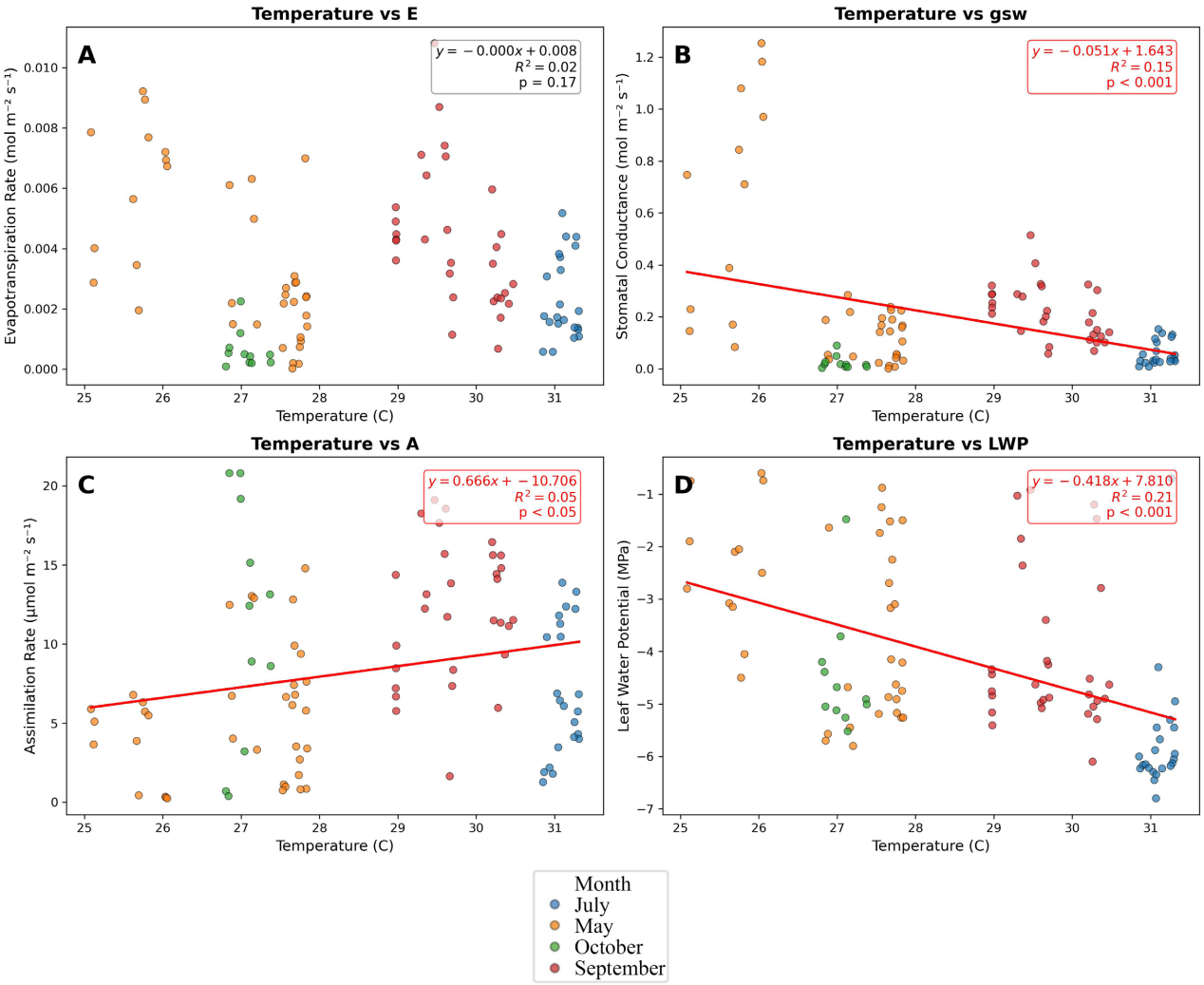

Figure 6. Temperature in Celsius was extracted from ERA5 land hourly from Google earth engine and resampled to minutes. Temperature values were paired with leaf measurements by time. Scatterplots depict temperature against transpiration (A), stomatal conductance (B), assimilation (C), and leaf water potential (D). The red line is the regression line indicating a significant relationship where the p-value is less than 0.05. The R-squared value, p-value, and trend line equation are represented in the box at the top right corner of each graph. Blue dots represent July, orange represents May, green represents October, and red represents September.

VPD explained about 12 percent of the variation in assimilation rate with a p-value < 0.001. There was a significant positive trend (y = 4.327x + 3.992) between VPD and assimilation rate (Figure 5, panel C).

VPD explained about 22 percent of the variation in LWP with a p-value < 0.001. There was a significant negative trend (y = −1.826x − 2.338) between VPD and LWP (Figure 5, panel D).

According to the linear regression analysis between temperature and transpiration, temperature explained about 2 percent of the variation in transpiration rate with a p-value of 0.17 signifying no significant trend between temperature and transpiration (Figure 6, panel A).

Temperature explained about 15 percent of the variation in stomatal conductance with a p-value < 0.001. There was a significant negative trend (y = −0.051x + 1.643) between temperature and stomatal conductance (Figure 6, panel B).

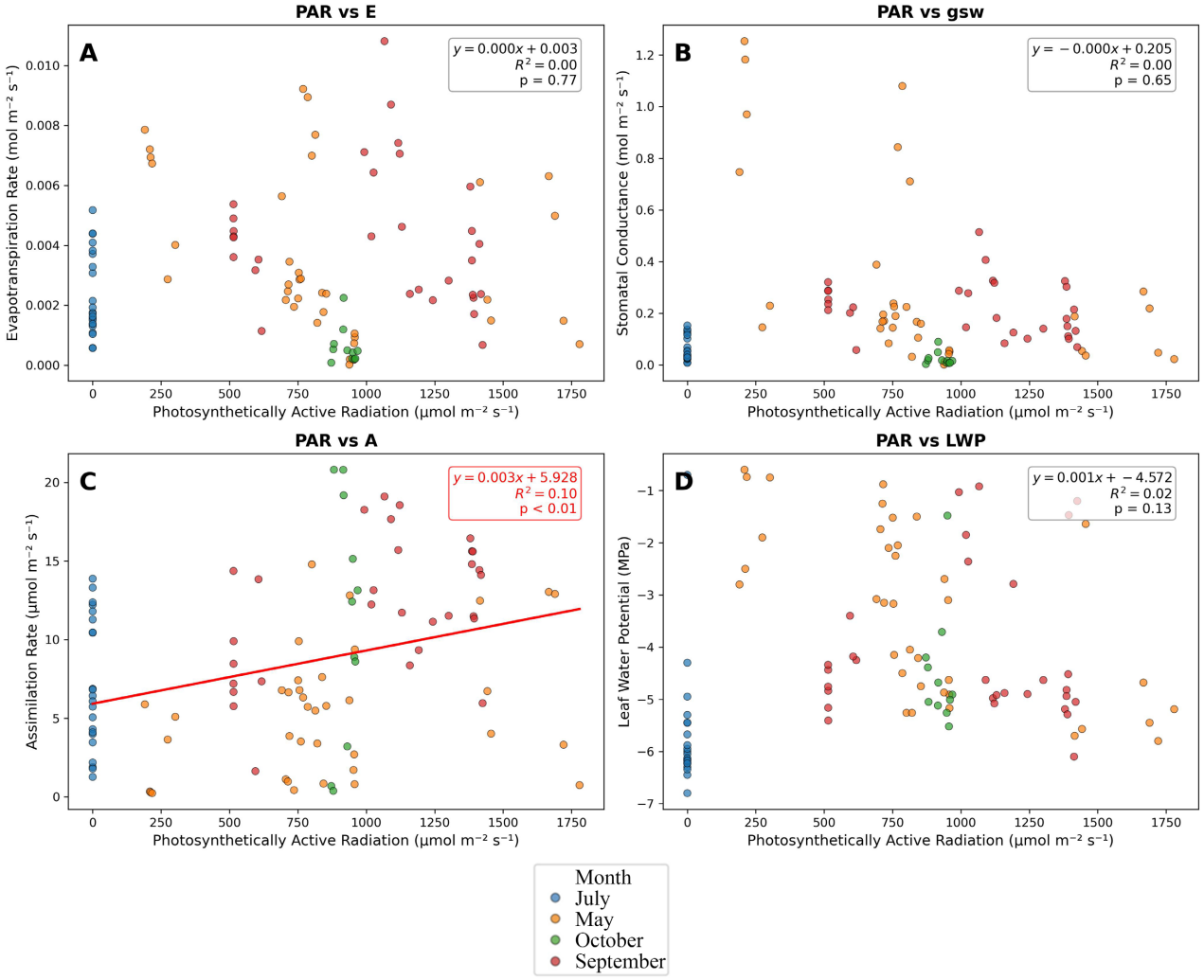

Figure 7. Photosynthetically active radiation (PAR) was extracted from ERA5 land hourly from Google earth engine and resampled to minutes. PAR values were paired with leaf measurements by time. Scatterplots depict PAR against transpiration (A), stomatal conductance (B), assimilation (C), and leaf water potential (D). The red line is the regression line indicating a significant relationship where the p-value is less than 0.05. The R-squared value, p-value, and trend line equation are represented in the box at the top right corner of each graph.

Temperature only explained about 0.05 of the variation in assimilation with a

slightly significant p-value of 0.02 and a positive trend (y = 0.666x – 10.706) (Figure 6, panel C).

Temperature explained about 21 percent of the variation in LWP with a p-value < 0.001. There was a significant negative trend (y = −0.418x + 7.810) between temperature and LWP (Figure 6, panel D).

According to the linear regression analysis for PAR, PAR did not explain any of the variation in transpiration, stomatal conductance, or LWP (Figure 7, panel A, B, D).

PAR explained only 10 percent of the variation in assimilation rate. With a p-value < 0.01, there was a significant positive trend (y = 0.003x + 5.928) between PAR and assimilation rate (Figure 7, panel C).

4. Discussion

We attempted to understand how different age classes of *Avicennia germinans* adapt their hydraulic strategies to maintain efficient photosynthesis under environmental fluctuations. Over the measurement period, atmospheric VPD increased corresponding to decreasing precipitation and high temperatures (Figure 4; Table 1). Therefore, the atmosphere exerted an increasingly negative water potential that tended to pull water out of the leaves through the stomatal openings. By measuring transpiration, assimilation, and stomatal conductance, we observed how the trees regulated their photosynthetic inputs in response to these increasingly stressful conditions.

4.1. Age Class Differences

We found that pre-freeze juveniles and post-freeze saplings did not significantly differ in most of their hydraulic responses to environmental changes. The exceptions were in October where juveniles experienced significantly more negative predawn LWP than saplings and where juveniles had significantly higher midday assimilation rates than saplings. Predawn water availability is primarily limited by salinity for mangroves. Therefore, this result is surprising as studies have shown younger trees to be more sensitive to salinity than older trees [22]. A possible explanation for this could be different rooting depths and variation of salt build-up at different soil depths [45] [46].

Juvenile and sapling *A. germinans* did not exhibit significant differences in stomatal conductance, transpiration or WUE. We expected saplings to have a higher WUE than juveniles because saplings have narrower xylem vessels [24] and lower salt tolerance [23] leading to lower water content. We expected this difficulty in water uptake would translate to strategies that would promote water retention against transpiration. Simultaneously, photosynthesis is especially important for the early growth and development of young mangroves [47]. Therefore, a high WUE is more essential for saplings than for juveniles. Instead, we observed consistent WUE across age classes and disturbance histories as well as similar increases in WUE in response to the higher VPD conditions in October (Figure 3,

panel D).

Overall, the consistency between juvenile and sapling *A. germinans* in their hydraulic strategies across variable environmental conditions, mostly clearly seen in their WUE, demonstrates consistent resilience across certain age classes and disturbance histories. High resilience is observed in young mangroves overall (juveniles and saplings) in their ability to adapt their hydraulic strategies to higher VPD conditions, particularly that they are able to increase their carbon assimilation without experiencing runaway water loss to the atmosphere (**Figure 5**).

The two age classes also reflected the pre-freeze and post-freeze *A. germinans* populations, and the consistency in WUE between the two groups shows evidence of physiological recovery or the lack of lingering freeze damage in the pre-freeze trees. This finding is supported by Osland *et al.*, (2015) who observed that saplings sustained the least freeze damage of all other age classes [25]. This helps explain the presence of healthy juveniles trees who were likely saplings during winter storm Uri in 2021.

An alternative explanation for the non-significant differences between sapling and juvenile hydraulic strategies is the relatively small difference in maximum height used to define each age class (65 cm for saplings and 100 cm for juveniles). While juveniles were not defined as having a maximum height of one meter, the extensively branched juvenile trees found at our field site did not exceed about one meter in height. Equipment constraints also limited us from measuring leaves from smaller saplings (particularly the gasket size of the pressure chamber seal). Future studies on the differences in age class hydraulic strategies should be conducted at a site with greater range in tree heights with a greater difference in maximum height for each age group. Future studies should also include adult mangroves (> 5 years old) to produce a more comprehensive understanding of age class differences in hydraulic strategies of *A. germinans*.

Our sample size is also a limitation as out of 9 - 12 samples per time of day, about 1/3 of our samples were identified as saplings and 2/3 were identified as juveniles.

The usage of height as a proxy for age is an assumption that is limited by varying growth rates of individual trees.

4.2. Hydraulic Trait Fluctuations

We saw a number of fluctuations in LWP, transpiration, carbon assimilation, and stomatal conductance over the course of the 2024 growing season.

Midday LWP was consistently more negative than predawn LWP, aligned with the expectation that plant stress increases as the day progresses.

We observed that hydraulic trait fluctuations, especially where we saw dramatic dips or spikes, corresponded more closely to the environmental conditions near the time we conducted leaf measurements rather than the monthly averages when the trend between monthly averages differed from that of the measurement period conditions (**Table 1**).

For example, the spike in transpiration and stomatal conductance in September corresponded with relatively higher precipitation (up to 0.31 mm) during the time immediately surrounding the September measurement period, even though the average monthly precipitation was lower than that of July (**Figure 3**; **Table 1**). We hypothesize that this peak is related to an increase in freshwater availability and humidity around the time the measurements were taken but is not necessarily reflected in the coarse resolution meteorological data.

Similarly, we observed a dramatic dip in midday LWP in July where precipitation was the second lowest (0.01 mm) and VPD was the second highest (1.20 kPa) of the four months behind October. July also had the highest temperature and the highest pore water salinity monthly average and during the measurement period. These compounding stresses are likely the reason that July experienced a dramatic dip in LWP (**Figure 2**) and stomatal conductance (**Figure 3**) but not October [48].

Notably, we observed consistent WUE across May, July, and September, but significantly higher WUE in October. This increase in WUE corresponded with the low transpiration rate and stomatal conductance and the higher CO_2 assimilation rate in October (**Figure 3**). LWP was on average more negative in October (**Figure 2**), which shows that although photosynthetic productivity did not wane with increasing VPD (**Figure 5**), the mangroves still experienced increasing water stress at the leaf level.

Ulatowski and Matheny (2025) observed that *A. germinans* moved from low (>2 kPa) to high (3 - 5 kPa) VPD conditions in a climate and salinity-controlled greenhouse experiment increased their WUE in the initial two days of exposure. After two days, prolonged exposure to high VPD caused declines in WUE with greater stomatal closure and decreased assimilation [48]. Similarly, under low but steadily increasing VPD in our field site, we observed increases in WUE and assimilation.

Our data supports the conclusions made by Reef and Lovelock (2015) and Ulatowski and Matheny (2025) that mangroves hydraulic traits are inherently plastic, moving from anisohydric behaviors to more isohydric to promote water conservation during periods of environmental stress [18] [48].

4.3. Environmental Influence

Of the environmental factors analyzed against hydraulic trait measurements (temperature, VPD, PAR), regression analyses showed that VPD had a stronger relationship with all of the measured traits than did temperature or PAR (**Figures 5-7**). Mangrove species are especially sensitive to changes in VPD and are known to adjust their stomatal openness to protect against water loss via evapotranspiration [18] [48]-[51].

As VPD increased at our field site, transpiration and stomatal conductance in the mangroves also decreased, indicating a closing of the stomata to reduce water loss. However, LWP continued to become more negative despite decreasing transpiration. LWP is a measure of the tension holding water inside the leaf with less

water availability resulting in increasing tension within the vessels. One would expect that with less water escaping via transpiration, leaf water availability would increase, resulting in a higher (less negative) LWP. Our results, however, run contrary to this assumption demonstrating that stomatal closure alone does not significantly alleviate highly negative LWP on short time scales (predawn to midday).

The VPD values we observed at our field site (0.23 - 1.84 kPa during measurement days (**Table 1**, panel B)) were lower than the threshold where VPD begins to affect mangrove productivity (2.50 - 2.95 kPa) according to Gou *et al.* (2024) [52]. Under these low VPD conditions, assimilation increased with VPD despite declining stomatal conductance, leading to the increase in WUE in October, the highest VPD month (**Figure 3**, **Table 1**). Even though the mangroves were not under high atmospheric stress, we still observed a stress response with the decline in stomatal conductance. As Ulatowski and Matheny (2025) showed, WUE would likely begin to decrease after exceeding the 2.50 - 2.95 kPa VPD threshold for a sustained period of time [48].

A number of studies have also observed the strong relationship between VPD and stomatal closure in general vegetation and in mangroves specifically [48]-[51]. A reanalysis of the data in Clough and Sim (1989) by Reef & Lovelock (2015) showed also that increasing sensitivity to VPD is positively correlated with higher stomatal conductance at low VPD. They also found that VPD sensitivity is higher in more salt tolerant species such as mangroves of the genus *Avicennia* [18] [21] [50] [53].

Another environmental factor that could have contributed to the increase in WUE in October is the decrease in temperature. The optimal air temperature for photosynthetic activity is 28˚C with photosynthesis being restricted when the air temperature falls below 10˚C or exceeds 35˚C [54]. The range of temperature at our site was 20.95˚C - 31.31˚C, reaching the highest in July at a range of 27.91˚C - 31.31˚C during the measurement period. Air temperatures steadily fell to a range of 20.95˚C - 27.38˚C during the measurement period in October, lowering temperature stress on the mangroves which may have promoted greater photosynthetic activity.

We also observed a moderately significant positive association between PAR and assimilation. While there was high variability in the values for PAR, it is likely that increasing PAR promoted higher assimilation rates as light availability drives photosynthesis.

The sample size of salinity data was not large enough to conduct any meaningful trend analysis but can be used to contextualize the root zone stress the plants were under at the time of measurement. Salinities greater than 40 ppt like those we observed (**Table 1**, panel B) can cause significant plant stress and stomatal closure [48] [55]. Because the mangroves at our field site were under moderate to high osmotic stress (35 - 45 ppt), it is likely that salinity compounded with VPD to induce the observed mangrove stress responses [48].

High VPD can lead to xylem cavitation, water stress, and reduced productivity

which in turn leads to reduction of growth in mangroves [50] [54]. Therefore, the ability of mangroves, especially in young, developing saplings, to maintain a high water-use efficiency as VPD increases is important for their survival, growth, and establishment. We see that even under low atmospheric stress, black mangroves will still close their stomata to reduce water loss but will simultaneously optimize photosynthesis through increasing assimilation.

4.4. Future Improvements

We conducted leaf-level measurements on a range of old and new growth mangrove leaves. Leaf age has been shown to influence mesophyll conductance and carbon assimilation [56]. Therefore, future studies using leaf measurements should strive to consistently measure leaves of similar maturity.

The short time frame of only four months across the summer growing season means that conclusions we can draw regarding water regulation plasticity across different environmental conditions are inherently limited to summer temperatures, PAR, and VPD. A clearer picture of hydraulic plasticity could be seen under higher variability in environmental conditions over the course of an entire year, encompassing all the seasonal variations in the temperate zone.

Better understanding of the relationship between PAR and hydraulic traits could be gained from using diffuse fraction of PAR instead of direct PAR [57].

5. Conclusions

Juvenile and sapling mangroves did not differ significantly in the majority of their water regulation and gas exchange strategies. Although we found that juveniles exhibited higher assimilation rates during the highest VPD month (October), they were still consistent with saplings in their WUE across all VPD conditions observed. We saw the highest WUE and greatest plant stress (LWP) during the highest VPD conditions. Hydraulic plasticity and high WUE, especially in the younger age class, may be an essential adaptation to continue to survive, expand, and establish in an increasingly changing climate where potential drought will bring prolonged atmospheric and osmotic stress. Overall, WUE was consistent between the pre- (sapling) and post-freeze (juvenile) age classes suggesting a lack of lingering freeze damage and the potential for population recovery after disturbance.

We found that VPD had a greater effect on transpiration, stomatal conductance, assimilation, and LWP, than temperature or PAR. We observed that under low VPD conditions (> 2 kPa), transpiration and stomatal conductance decreased while CO_2 assimilation increased with increasing VPD. This is in line with the study by Ulatowski and Matheny (2025) that showed that *A. germinans* increase their WUE under short term VPD stress [48].

We conclude that *A. germinans* are resilient to some seasonal shifts in temperature and VPD by adjusting their hydraulic strategies on monthly time scales. We also conclude that the *A. germinans* are resilient to extreme freezing events by recovering a healthy, hydraulically plastic population through surviving saplings.

With predictions of increasing drought brought on by climate change [58] [59], survival of mangrove forests will depend on this ability to adapt to stressful environmental conditions. As mangrove populations push their ranges further into the temperate zones, their plasticity in water regulation will be tested by seasonal changes in environmental conditions. Understanding the hydraulic strategies of these vulnerable yet resilient trees will help us to prepare for foreseeable threats to their existence by climate change or human activity.

Acknowledgements

AMM, CG, CC, and MUU were supported by the Department of Energy Terrestrial Ecosystem Science Program Grant (DE-SC0020116) and in part by NSF CAREER Award 2046768.

Conflicts of Interest

The authors declare no conflicts of interest regarding the publication of this paper.

References

[1] Saintilan, N., Wilson, N.C., Rogers, K., Rajkaran, A. and Krauss, K.W. (2013) Mangrove Expansion and Salt Marsh Decline at Mangrove Poleward Limits. *Global Change Biology*, **20**, 147-157. https://doi.org/10.1111/gcb.12341

[2] Armitage, A.R., Highfield, W.E., Brody, S.D. and Louchouarn, P. (2015) The Contribution of Mangrove Expansion to Salt Marsh Loss on the Texas Gulf Coast. *PLOS ONE*, **10**, e0125404. https://doi.org/10.1371/journal.pone.0125404

[3] Bardou, R., Osland, M.J., Scyphers, S., Shepard, C., Aerni, K.E., Alemu I, J.B., *et al.* (2023) Rapidly Changing Range Limits in a Warming World: Critical Data Limitations and Knowledge Gaps for Advancing Understanding of Mangrove Range Dynamics in the Southeastern Usa. *Estuaries and Coasts*, **46**, 1123-1140. https://doi.org/10.1007/s12237-023-01209-7

[4] Langston, A.K. and Kaplan, D.A. (2020) Modelling the Effects of Climate, Predation, and Dispersal on the Poleward Range Expansion of Black Mangrove (*Avicennia germinans*). *Ecological Modelling*, **434**, Article ID: 109245. https://doi.org/10.1016/j.ecolmodel.2020.109245

[5] Osland, M.J., Day, R.H. and Michot, T.C. (2020) Frequency of Extreme Freeze Events Controls the Distribution and Structure of Black Mangroves (*Avicennia germinans*) near Their Northern Range Limit in Coastal Louisiana. *Diversity and Distributions*, **26**, 1366-1382. https://doi.org/10.1111/ddi.13119

[6] Osland, M.J., Day, R.H., Hall, C.T., Brumfield, M.D., Dugas, J.L. and Jones, W.R. (2016) Mangrove Expansion and Contraction at a Poleward Range Limit: Climate Extremes and Land-Ocean Temperature Gradients. *Ecology*, **98**, 125-137. https://doi.org/10.1002/ecy.1625

[7] Matheny, A.M., Restrepo Acevedo, A.M., Ulatowski, M. and Cabraal, S.A. (2022) Investigating the Impact of Winter Storm Uri on US Gulf Coast Estuaries [Poster Presentation]. *Frontiers in Hydrology Meeting*, San Juan, 19-24 June 2022. https://agu.confex.com/agu/hydrology22/meetingapp.cgi/Paper/1028082

[8] Liang, S., Zhou, R., Dong, S. and Shi, S. (2008) Adaptation to Salinity in Mangroves: Implication on the Evolution of Salt-Tolerance. *Science Bulletin*, **53**, 1708-1715.

https://doi.org/10.1007/s11434-008-0221-9

[9] Mahadik, S.S., Ghosh, S. and Banerjee, S. (2022) Mangroves as Potential Agents of Phytoremediation: A Review. *Research Journal of Chemistry and Environment*, **26**, 150-156. https://doi.org/10.25303/2609rjce1500156

[10] Menéndez, P., Losada, I.J., Torres-Ortega, S., Narayan, S. and Beck, M.W. (2020) The Global Flood Protection Benefits of Mangroves. *Scientific Reports*, **10**, Article No. 4404. https://doi.org/10.1038/s41598-020-61136-6

[11] Samarah, N.H. (2005) Effects of Drought Stress on Growth and Yield of Barley. *Agronomy for Sustainable Development*, **25**, 145-149. https://doi.org/10.1051/agro:2004064

[12] Farooq, M., Wahid, A., Kobayashi, N., Fujita, D. and Basra, S.M.A. (2009) Plant Drought Stress: Effects, Mechanisms and Management. In: Lichtfouse, E., Navarrete, M., Debaeke, P., Véronique, S. and Alberola, C., Eds., *Sustainable Agriculture*, Springer, 153-188. https://doi.org/10.1007/978-90-481-2666-8_12

[13] Ewers, F.W., Lopez-Portillo, J., Angeles, G. and Fisher, J.B. (2004) Hydraulic Conductivity and Embolism in the Mangrove Tree *Laguncularia racemosa*. *Tree Physiology*, **24**, 1057-1062. https://doi.org/10.1093/treephys/24.9.1057

[14] Sperry, J.S. and Tyree, M.T. (1988) Mechanism of Water Stress-Induced Xylem Embolism. *Plant Physiology*, **88**, 581-587. https://doi.org/10.1104/pp.88.3.581

[15] Buckley, T.N. (2005) The Control of Stomata by Water Balance. *New Phytologist*, **168**, 275-292. https://doi.org/10.1111/j.1469-8137.2005.01543.x

[16] Sparks, J.P. and Black, R.A. (1999) Regulation of Water Loss in Populations of *Populus trichocarpa*: The Role of Stomatal Control in Preventing Xylem Cavitation. *Tree Physiology*, **19**, 453-459. https://doi.org/10.1093/treephys/19.7.453

[17] Hochberg, U., Rockwell, F.E., Holbrook, N.M. and Cochard, H. (2018) Iso/Anisohydry: A Plant-Environment Interaction Rather than a Simple Hydraulic Trait. *Trends in Plant Science*, **23**, 112-120. https://doi.org/10.1016/j.tplants.2017.11.002

[18] Reef, R. and Lovelock, C.E. (2014) Regulation of Water Balance in Mangroves. *Annals of Botany*, **115**, 385-395. https://doi.org/10.1093/aob/mcu174

[19] Matheny, A.M., Mirfenderesgi, G. and Bohrer, G. (2017) Trait-Based Representation of Hydrological Functional Properties of Plants in Weather and Ecosystem Models. *Plant Diversity*, **39**, 1-12. https://doi.org/10.1016/j.pld.2016.10.001

[20] Feldman, A.F., Short Gianotti, D.J., Konings, A.G., Gentine, P. and Entekhabi, D. (2021) Patterns of Plant Rehydration and Growth Following Pulses of Soil Moisture Availability. *Biogeosciences*, **18**, 831-847. https://doi.org/10.5194/bg-18-831-2021

[21] Ball, M. (1988) Salinity Tolerance in the Mangroves *Aegiceras corniculatum* and *Avicennia marina*. I. Water Use in Relation to Growth, Carbon Partitioning, and Salt Balance. *Functional Plant Biology*, **15**, 447-464. https://doi.org/10.1071/pp9880447

[22] Dittmann, S., Mosley, L., Stangoulis, J., Nguyen, V.L., Beaumont, K., Dang, T., *et al.* (2022) Effects of Extreme Salinity Stress on a Temperate Mangrove Ecosystem. *Frontiers in Forests and Global Change*, **5**, Article ID: 859283. https://doi.org/10.3389/ffgc.2022.859283

[23] Kodikara, K.A.S., Jayatissa, L.P., Huxham, M., Dahdouh-Guebas, F. and Koedam, N. (2017) The Effects of Salinity on Growth and Survival of Mangrove Seedlings Changes with Age. *Acta Botanica Brasilica*, **32**, 37-46. https://doi.org/10.1590/0102-33062017abb0100

[24] Cisneros-de la Cruz, D.J., Yáñez-Espinosa, L., Reyes-García, C., Us-Santamaría, R. and Andrade, J.L. (2021) Hydraulic Architecture of Seedlings and Adults of *Rhi-*

zophora mangle L. in Fringe and Scrub Mangrove. *Botanical Sciences*, **100**, 370-382. https://doi.org/10.17129/botsci.2906

[25] Osland, M.J., Day, R.H., From, A.S., McCoy, M.L., McLeod, J.L. and Kelleway, J.J. (2015) Life Stage Influences the Resistance and Resilience of Black Mangrove Forests to Winter Climate Extremes. *Ecosphere*, **6**, 1-15. https://doi.org/10.1890/es15-00042.1

[26] Guo, P., Lin, Y., Du, L., Gu, X., Deng, Y., Wang, W., *et al.* (2025) Long-Term Vegetation Succession Increases Aquatic Animal Structural Stability and Functional Vulnerability Following Pond-to-Mangrove Restoration. *Global Ecology and Conservation*, **62**, e03838. https://doi.org/10.1016/j.gecco.2025.e03838

[27] Peng, Y., Wang, Q. and Bai, L. (2020) Identification of the Key Landscape Metrics Indicating Regional Temperature at Different Spatial Scales and Vegetation Transpiration. *Ecological Indicators*, **111**, Article ID: 106066. https://doi.org/10.1016/j.ecolind.2020.106066

[28] Williams, I.N. and Torn, M.S. (2015) Vegetation Controls on Surface Heat Flux Partitioning, and Land-Atmosphere Coupling. *Geophysical Research Letters*, **42**, 9416-9424. https://doi.org/10.1002/2015gl066305

[29] Leal, M. and Spalding, M.D. (2024) The State of the World's Mangroves 2024. Global Mangrove Alliance. https://doi.org/10.5479/10088/119867

[30] Ashton, E.C. (2022) Threats to Mangroves and Conservation Strategies. In: Das, S.C., Pullaiah and Ashton, E.C., Eds., *Mangroves: Biodiversity, Livelihoods and Conservation*, Springer, 217-230. https://doi.org/10.1007/978-981-19-0519-3_10

[31] Kumar, A., Anju, T., Archa, V., Warrier, V.P., Kumar, S., Goud, G.S., *et al.* (2021) Mangrove Forests: Distribution, Species Diversity, Roles, Threats and Conservation Strategies. In: Sharma, S. and Singh, P., Eds., *Wetlands Conservation*, Wiley, 229-271. https://doi.org/10.1002/9781119692621.ch12

[32] International Union for Conservation of Nature (n.d.) Red List of Mangrove Ecosystems. https://www.iucn.org/resources/conservation-tool/iucn-red-list-ecosystems/red-list-mangrove-ecosystems

[33] Loving, M. (2023) Assessing the Effect of Pollution on *Rhizophora mangle* in Jamaica: A Comparative Study. Master's Thesis, The University of Texas. https://doi.org/10.26153/tsw/48562

[34] Lefcheck, J.S., Hughes, B.B., Johnson, A.J., Pfirrmann, B.W., Rasher, D.B., Smyth, A.R., *et al.* (2019) Are Coastal Habitats Important Nurseries? A Meta-Analysis. *Conservation Letters*, **12**, e12645. https://doi.org/10.1111/conl.12645

[35] Choudhary, B., Dhar, V. and Pawase, A.S. (2024) Blue Carbon and the Role of Mangroves in Carbon Sequestration: Its Mechanisms, Estimation, Human Impacts and Conservation Strategies for Economic Incentives. *Journal of Sea Research*, **199**, Article ID: 102504. https://doi.org/10.1016/j.seares.2024.102504

[36] Huang, R., He, J., Wang, N., Christakos, G., Gu, J., Song, L., *et al.* (2023) Carbon Sequestration Potential of Transplanted Mangroves and Exotic Saltmarsh Plants in the Sediments of Subtropical Wetlands. *Science of the Total Environment*, **904**, Article ID: 166185. https://doi.org/10.1016/j.scitotenv.2023.166185

[37] Chatting, M., Al-Maslamani, I., Walton, M., Skov, M.W., Kennedy, H., Husrevoglu, Y.S., *et al.* (2022) Future Mangrove Carbon Storage under Climate Change and Deforestation. *Frontiers in Marine Science*, **9**, Article ID: 781876. https://doi.org/10.3389/fmars.2022.781876

[38] Othman, M.A. (1994) Value of Mangroves in Coastal Protection. *Hydrobiologia*, **285**, 277-282. https://doi.org/10.1007/bf00005674

[39] LI-COR Biosciences (2016) LI-6800 Portable Photosynthesis System [Scientific Instrument]. LI-COR Biosciences. https://www.licor.com/products/photosynthesis/LI-6800

[40] PMS Instrument Company (2011) Model 600D Pressure Chamber Instrument [Scientific Instrument]. PMS Instrument Company. https://www.pmsinstrument.com/products/model-600d/

[41] Beauzamy, L., Nakayama, N. and Boudaoud, A. (2014) Flowers under Pressure: Ins and Outs of Turgor Regulation in Development. *Annals of Botany*, **114**, 1517-1533. https://doi.org/10.1093/aob/mcu187

[42] Serval (n.d.) Refrigerated Automatic Centrifuge, Model 06930 [Scientific Instrument]. Thermo Fisher Scientific (Serval Division).

[43] Reichert Technologies (n.d.) Optical Refractometer [Scientific Instrument]. AMETEK, Inc.

[44] Muñoz Sabater, J. (2019) ERA5-Land Monthly Averaged Data from 1981 to Present. Copernicus Climate Change Service (C3S) Climate Data Store (CDS). https://doi.org/10.24381/cds.68d2bb30

[45] Wang, F., Yang, S., Wei, Y., Shi, Q. and Ding, J. (2021) Characterizing Soil Salinity at Multiple Depth Using Electromagnetic Induction and Remote Sensing Data with Random Forests: A Case Study in Tarim River Basin of Southern Xinjiang, China. *Science of the Total Environment*, **754**, Article ID: 142030. https://doi.org/10.1016/j.scitotenv.2020.142030

[46] Arnaud, M., Morris, P.J., Baird, A.J., Dang, H. and Nguyen, T.T. (2021) Fine Root Production in a Chronosequence of Mature Reforested Mangroves. *New Phytologist*, **232**, 1591-1602. https://doi.org/10.1111/nph.17480

[47] Krauss, K.W., Lovelock, C.E., McKee, K.L., López-Hoffman, L., Ewe, S.M.L. and Sousa, W.P. (2008) Environmental Drivers in Mangrove Establishment and Early Development: A Review. *Aquatic Botany*, **89**, 105-127. https://doi.org/10.1016/j.aquabot.2007.12.014

[48] Ulatowski, M. and Matheny, A.M. (2025) Compounding Environmental Stressors Cause Governing Hydraulic Behaviours to Shift from Roots to Leaves in *Avicennia germinans*. *Ecohydrology*, **18**, e70080. https://doi.org/10.1002/eco.70080

[49] Oren, R., Sperry, J.S., Katul, G.G., Pataki, D.E., Ewers, B.E., Phillips, N., *et al.* (1999) Survey and Synthesis of Intra- and Interspecific Variation in Stomatal Sensitivity to Vapour Pressure Deficit. *Plant, Cell & Environment*, **22**, 1515-1526. https://doi.org/10.1046/j.1365-3040.1999.00513.x

[50] Clough, B.F. and Sim, R.G. (1989) Changes in Gas Exchange Characteristics and Water Use Efficiency of Mangroves in Response to Salinity and Vapour Pressure Deficit. *Oecologia*, **79**, 38-44. https://doi.org/10.1007/bf00378237

[51] Ball, M.C., Cochrane, M.J. and Rawson, H.M. (1997) Growth and Water Use of the Mangroves *Rhizophora apiculata* and *R. stylosa* in Response to Salinity and Humidity under Ambient and Elevated Concentrations of Atmospheric CO_2. *Plant, Cell & Environment*, **20**, 1158-1166. https://doi.org/10.1046/j.1365-3040.1997.d01-144.x

[52] Gou, R., Chi, J., Liu, J., Luo, Y., Shekhar, A., Mo, L., *et al.* (2024) Atmospheric Water Demand Constrains Net Ecosystem Production in Subtropical Mangrove Forests. *Journal of Hydrology*, **630**, Article ID: 130651. https://doi.org/10.1016/j.jhydrol.2024.130651

[53] Ye, Y., Tam, N.F.-Y., Lu, C.-Y. and Wong, Y.-S. (2005) Effects of Salinity on Germination, Seedling Growth and Physiology of Three Salt-Secreting Mangrove Species. *Aquatic Botany*, **83**, 193-205. https://doi.org/10.1016/j.aquabot.2005.06.006

[54] Zheng, Y. and Takeuchi, W. (2022) Estimating Mangrove Forest Gross Primary Production by Quantifying Environmental Stressors in the Coastal Area. *Scientific Reports*, **12**, Article No. 2238. https://doi.org/10.1038/s41598-022-06231-6

[55] Biber, P.D. (2006) Measuring the Effects of Salinity Stress in the Red Mangrove, *Rhizophora mangle* L. *African Journal of Agricultural Research*, **1**, 1-4. https://aquila.usm.edu/cgi/viewcontent.cgi?article=3298&context=fac_pubs

[56] Jahan, E., Sharwood, R.E. and Tissue, D.T. (2023) Effects of Leaf Age during Drought and Recovery on Photosynthesis, Mesophyll Conductance and Leaf Anatomy in Wheat Leaves. *Frontiers in Plant Science*, **14**, Article ID: 1091418. https://doi.org/10.3389/fpls.2023.1091418

[57] Chen, F., Yang, X., Yu, Q. and Han, B. (2024) Quantifying the Effects of Diffuse Photosynthetically Active Radiation on Water Use Efficiency in Different Ecosystems. *Agricultural and Forest Meteorology*, **356**, Article ID: 110191. https://doi.org/10.1016/j.agrformet.2024.110191

[58] Cook, B.I., Mankin, J.S. and Anchukaitis, K.J. (2018) Climate Change and Drought: From Past to Future. *Current Climate Change Reports*, **4**, 164-179. https://doi.org/10.1007/s40641-018-0093-2

[59] Kim, T.-W. and Jehanzaib, M. (2020) Drought Risk Analysis, Forecasting and Assessment under Climate Change. *Water*, **12**, Article No. 1862. https://doi.org/10.3390/w12071862